Materials Science and Technology

ISSN: 0267-0836 (Print) 1743-2847 (Online) Journal homepage: https://www.tandfonline.com/loi/ymst20

Application of low M_s temperature consumable to dissimilar welded joint

D. L. Saraiva, M. Béreš, C. C. Silva, C. S. Nunes, J. J. M. Silva & H. F. G. Abreu

To cite this article: D. L. Saraiva, M. Béreš, C. C. Silva, C. S. Nunes, J. J. M. Silva & H. F. G. Abreu (2014) Application of low M_s temperature consumable to dissimilar welded joint, Materials Science and Technology, 30:9, 1057-1062, DOI: 10.1179/1743284714Y.0000000516

To link to this article: https://doi.org/10.1179/1743284714Y.0000000516

Published online: 27 Feb 2014.

Application of low M_S temperature consumable to dissimilar welded joint

D. L. Saraiva, M. Béreš, C. C. Silva, C. S. Nunes, J. J. M. Silva and H. F. G. Abreu*

The welding of dissimilar joints is very common in systems used in oil exploration and production in deep sea waters. Commonly involves welding of low carbon steel pipes with low alloy steel forgings both with inner Inconel clad. The forged steel part undergoes a process of buttering with Inconel or carbon steel electrode before the weld of the joint. The buttering process is followed by a process of residual stresses relief. The conventional way of reducing the level of residual stresses in welded joints is to apply post welding heat treatments. Depending on the size and complexity of the parts to be joined, this can become a serious problem. An alternative technique for reducing residual stresses is to use an electrode that during the cooling process undergoes a displacive transformation at a relatively low temperature so that the deformation resulting from the transformation compensates the contraction during the cooling process, and, although many papers have been published in this direction using Fe–Cr–Ni alloys, most of them report a loss of toughness in the weld metal. Maraging steel is a family of materials with M_S temperature below 200°C and even without the final heat treatment of aging has superior mechanical properties to low alloy steels used in forgings. In this work, forged piece of AISI 4130 was buttered with Maraging 350 weld consumable and subsequently welded to ASTM A36 steel using Inconel 625 filler metal. In addition, the dissimilar base metal plates were welded together using Maraging 350 steel weld consumable. The levels of residual stress, and the toughness and microstructures of heat affected zone and weld metal were investigated.

Keywords: Low transformation temperature, Residual stress, Welding, Martensitic transformation

This paper is part of a special issue on Adventures in the Physical Metallurgy of Steels

Introduction

Dissimilar metal welding is widely used in power generation and aerospace industries in addition to subsea oil and gas systems.[1,2] In the latter, components such as forged hubs or tees made of low alloy steels are typically buttered with a carbon steel or nickel alloy weld consumable which is usually followed by a residual stress relief treatment and finally welded to an high strength low alloy steel pipe.[2] Residual tensile stresses induced by welding are of concern because they can promote stress corrosion cracking, reduce fatigue and static strength, or can give rise to distortion.[3] Stress relieving can be carried out by a post-weld heat treatment, although for large welded structures the applicability of such stress mitigation technique might be impractical. Therefore, there has been great interest in minimising these stresses by use of weld consumables which undergo a displacive transformation (e.g. austenite→martensite/bainite/acicular ferrite) at a low temperature typically around 200–400°C where thermal stresses accumulated during cooling of the solidified weld metal are compensated by a deformation caused by this solid state phase transformation.

During cooling of the solidified weld metal, austenite may or may not decompose according to one of the following scenarios:

(i) reconstructive transformation, e.g. in conventional carbon steel weld filler
(ii) displacive transformation, e.g. in a low transformation temperature weld metal
(iii) no phase transformation, e.g. in a nickel based alloy consumable.

This phase transformation behaviour can significantly affect accumulation of stresses during welding.[4,5] The diffusion controlled reconstructive transformation mechanism in steels e.g. austenite→ferrite/pearlite is an isotropic volume change and takes place at higher temperatures typically around 500–650°C. In contrast, the anisotropic volumetric change during displacive transformation at lower temperatures is larger since this involves an invariant plane strain shape deformation with a large shear parallel to the invariant plane and a dilatation normal to the plane.[6] In addition, when displacive transformation takes place in welds a variant selection can occur where certain crystallographic variants are favoured. This may affect residual stress state to a

Department of Materials and Metallurgical Engineering, Federal University of Ceará – UFC, Fortaleza, CE, Brazil

*Correspondence author, email hamilton@ufc.br

Published by Maney on behalf of the Institute
Received 1 October 2013; accepted 22 January 2014
DOI 10.1179/1743284714Y.0000000516

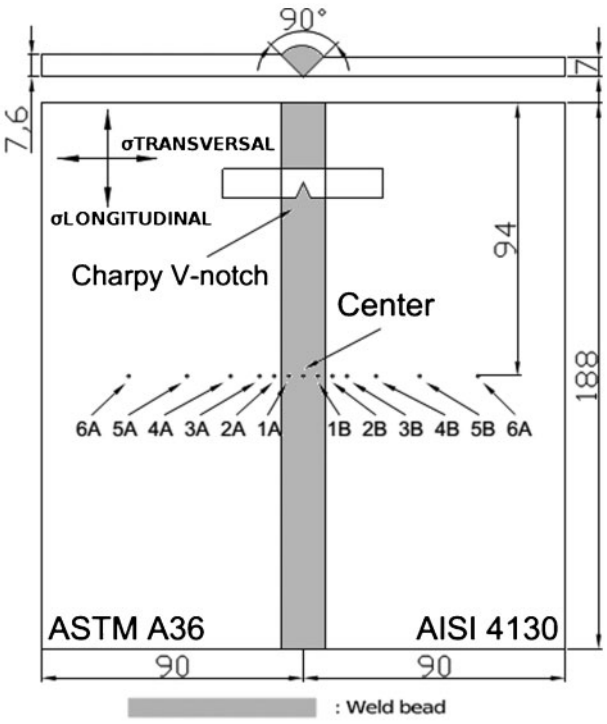

Distance from center (mm)					
1A	**2A**	**3A**	**4A**	**5A**	**6A**
5	10	15	25	40	60
1B	**2B**	**3B**	**4B**	**5B**	**6B**
5	10	15	25	40	60

1 Schematic representation of welded sample showing residual stresses measurement points where 1A indicates measurement point and 5 the distance from weld centreline in mm. Also depicted is position of Charpy V-notch specimen

greater extent than any volume changes, since the shear component of the associated deformation is significantly larger than the dilatational component.[6–8]

A substantial body of modelling and experimental work has been carried out to demonstrate the effect of this transformation on residual stresses in ferritic[3,9] and austenitic[10,11] steels. During the last two decades, low transformation temperature (LTT) welding filler alloys have been developed.[12–19] Typically these Fe based alloys contain 0–15 wt-%Ni in addition to 0–15 wt-%Cr. Although these weld consumables reduced tensile residual stresses in the welded components and significantly improved their fatigue strength, in many cases the fracture toughness was found to be insufficient.

Here, the authors propose to utilise a commercial 18Ni maraging steel weld consumable in the gas tungsten arc welding (GTAW) process. Maraging steels have superior mechanical properties including satisfactory fracture toughness[20] combined with good corrosion resistance and weldeability and undergo solid state phase transformation at a low temperature ypically around 200°C. These low carbon high strength steels are alloyed with substitutional elements such as nickel, cobalt and molybdenum which produce precipitation hardening in martensite upon ageing. In the present study, dissimilar ferritic steel plates were joined by a butt weld, employing a maraging steel weld filler in addition to a nickel based weld consumable. Post-weld analysis revealed the effect of these weld consumables on residual stresses and mechanical properties.

Experimental procedure

Weld fabrication

In this study, the welded joints were designed with two dissimilar steel plates using AISI 4130 low alloy steel and ASTM A36 carbon structural steel with dimensions shown in Fig. 1. Prior to welding, the AISI 4130 steel plates were austenitised at 850°C for 10 min then quenched in water and finally tempered at 650°C for 2 h. The ASTM A36 plate was used in as delivered condition. In the welding process, two different weld consumables were used AWS ER NiCrMo-3 Ni based alloy (Inconel 625) wire with 1·2 mm diameter and GSCO12 maraging 350 steel wire with 0·8 mm diameter. The chemical composition of steel sheets and weld consumables is presented in Table 1 and their mechanical properties are shown in Table 2.[21–24]

The V-groove geometry with 45° for both plates was applied for all tested conditions. The welds were performed using gas tungsten arc welding (GTAW) cold wire feed process. An automatic workbench with a XY coordinator table and electronic power supply in addition to an automatic wire feeder with data acquisition system were employed in the process. The welds were performed in the flat position (1G) using a fixing table to constraint the weld shrinkage during the cooling. Argon 99·9% at a flowrate of 20 L min^{-1} was used as shielding and purge gas. An additional argon flow line was also used to purge the root.

Table 1 Chemical composition of base metal plates and weld consumables/wt-%

	C	Si	Mn	Ni	Cr	Mo	Fe	Nb	Co	Ti
AISI 4130 base metal	0·29	0·29	0·57	0·25	0·99	0·25	Bal.	…	…	…
ASTM A36 base metal	0·25	0·4	0·8	…	…	…	Bal.	…	…	…
ER NiCrMo-3 weld filler	0·011	0·05	0,01	64·43	22·2	9·13	0·19	3·5	…	…
GSCO 12 weld filler	0·02	0·03	0·02	18	…	4	Bal.	…	12	0·1

Table 2 Mechanical properties of base metal plates and weld consumables.[21–24]

	Yield strength/MPa	Tensile strength/MPa
AISI 4130 base metal	655	841
ASTM A36 base metal	220	400
ER NiCrMo-3 weld filler	590	760
GSCO 12 weld filler	827	1140

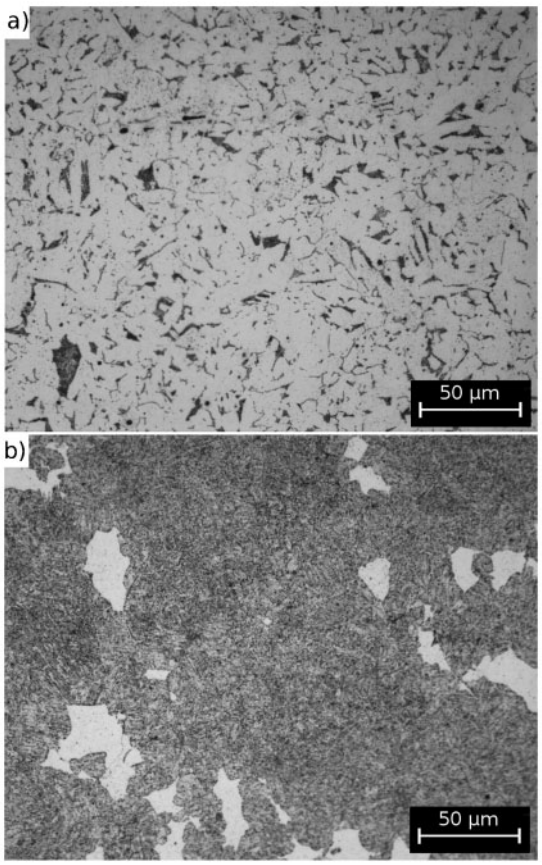

a ASTM A36; *b* AISI 4130

2 Optical micrographs showing microstructure of base metal plates

The methodology established for this study consisted in the production of two distinct welded joints with different combination of filler metals, as described below. For the first condition, Sample A, the AISI 4130 steel plate was buttered using the GSCO12 maraging steel weld consumable. For this, four parallel passes were required. After the buttering layer was deposited, the plate was machined to remove the excess of surface irregularities maintaining the 45° semi-V groove geometry. The thickness of the buttered layer after machining was ~2 mm. Finally, the plate was joined to the ASTM A36 steel plate using the AWS ER NiCrMo-3 filler metal. The second condition, Sample B, was produced without buttering and the dissimilar metal plates were joined employing the GSCO12 maraging steel weld consumable only. The welding parameters, together with number of passess are presented in Table 3.

X-ray residual stress measurements

After welding, residual stresses were measured by X-ray diffraction technique by the $\sin^2\psi$-method[25] based on the Bragg's Law using portable X-ray stress analyser XStress3000. The experimental parameters used in this study were: radiation source voltage 25 kV, current 6 mA, Cr K_α radiation ($\lambda_{CrK\alpha}$=2·29092 Å) which produces diffraction peak at 2θ=156° diffracting the bcc {211} plane of both base metal plates and maraging steel consumable respectively. Because of the austenitic fcc lattice structure of nickel based weld consumable, a Cr K_β radiation ($\lambda_{CrK\beta}$=2·08480 Å) and a detector angle 2θ of 158°, diffracting the {311} plane, were used. Measurements were performed at five ψ-angles (ψ=0, 20, 30, 40 and 45°). The analysis was carried out at the mid-length of both samples in the longitudinal and transversal direction at 13 measurement points at the top surface as indicated in Fig. 1. In this figure the dimensions of the welded plates are also shown.

Microstructural evaluation and mechanical testing

After the residual stress measurements were completed, ~10 mm thick slices containing the weld, heat affected zone and parent material were cut from the welded plates and prepared for metallographic analysis. This consisted of grinding with silicon carbide paper 120–1200 grit sequence, followed by mechanical polishing down to 1 μm diamond suspension. To reveal the microstructure of the dissimilar materials a variety of etching procedures were applied. For base metal plates an immersion etching with 5% nital was used. Fusion zone of plate welded with GSCO12 filer metal was etched with Marble's reagent. The Ni based alloy weld metal (AWS ER NiCrMo-3) specimens were subjected to an electrolytic etching with aqueous solution (10 wt-%) of chromic acid, applying a potential difference of 2 V for 15 s.

To determine fracture toughness of welds produced using the GSCO12 maraging steel filler, Charpy impact tests were conducted at room temperature. For this purpose, sub- sized $5 \times 10 \times 55$ mm Charpy V-notch specimens were extracted and machined in transversal direction from the plate B containing weld fusion zone in the mid-length of the specimens (Fig. 1).

Results and discussion

Microstructure

Typical ferritic–perlitic microstructure of ASTM A36 steel with average grain size of 15 μm is presented in Fig. 2*a*. The microstructure of AISI 4130 base metal

Table 3 Welding parameters

	Sample A			Sample B	
	Buttering weld* (4 parallel weld beads)	Root weld† (2 weld beads)	Completion weld† (8 weld beads)	Root weld* (2 weld beads)	Completion weld* (8 weld beads)
Voltage/V	14·0	14·5	13·5	15·0	15·5
Current/A	−170	−170	−170	−170	−235
Weld speed/mm min^{-1}	180	200	200	200	200
Weld wire speed/m min^{-1}	2·7–3·8	1·0–2·3	1·0	1·5	1·5–3·1

*Filler material: GSCO12 maraging steel.
†Filler material: AWS ER NiCrMo-3 nickel based alloy.

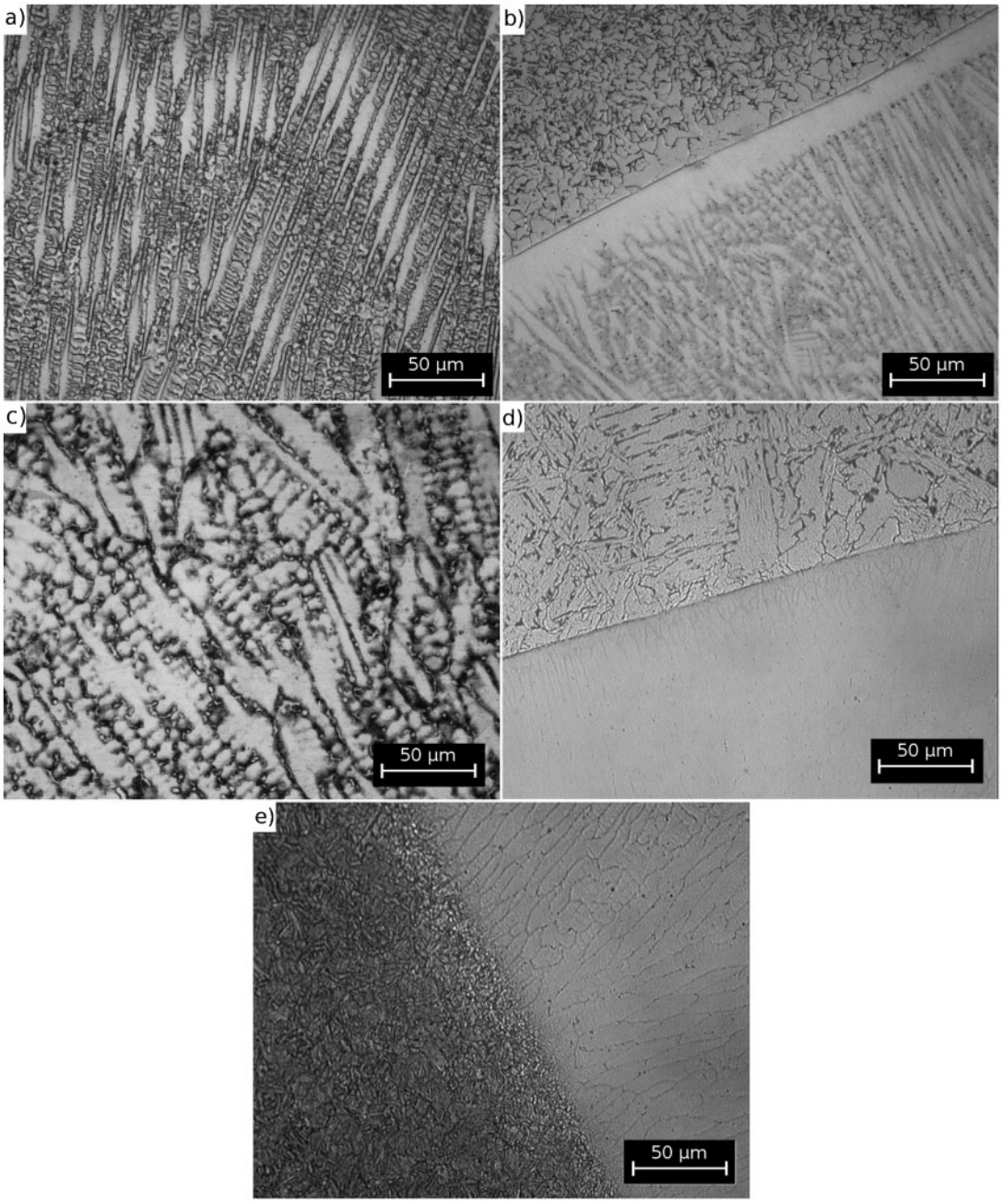

3 Optical micrographs showing microstructure of *a* fusion zone using AWS ER NiCrMo-3 consumable, *b* interface fusion zone AWS ER NiCrMo-3 consumable and ASTM A36 steel in mid-thickness of plate, *c* fusion zone using GSCO12 consumable, *d* interface using GSCO12 consumable and ASTM A36 steel in mid-thickness of plate, *e* interface fusion zone GSCO12 consumable and AISI 4130 steel in mid-thickness of plate

(Fig. 2*b*) consists of ferrite (bright) and tempered martensite (dark areas).

Microstructure of different regions in the welded plates revealed by optical microscopy is presented in Fig. 3. In the fusion zone of specimen welded with AWS ER NiCrMo-3 consumable (Fig. 3*a*) dendrites with dendritic arm spacing in 10–20 μm range and microsegregation in the interdendritic regions were identified. In the fusion zone of specimen welded with GSCO12 consumable, cellular dendritic grain microstructure with dendritic arm spacing in 5–15 μm range and microsegregation in the interdendritic regions were observed (Fig. 3*c*). The interfaces fusion zone: AISI 4130 and ASTM A36 steels shows microstructure subjected to thermal cycle during multipass welding. The thermal cycling caused reduction in grain size in both materials (Figure 3*b*, *d* and *e*).

The microsegregation in interdendritic regions could be identified in backscattered electron micrographs of fusion zone sample A (Fig. 4*a*) and in the sample B (Fig. 4*b*).

The impact toughness (normalised by the specimen net section area) determined in the fusion zone of sample B was 52 J cm^{-2} at RT. Please note that impact value of e.g. 18Ni-250 maraging steel (which belongs to the same class of material) can exceed 100% of the material used in the present research.[20] Therefore, 18Ni-250 maraging steel can be employed for applications with higher fracture toughness requirements.

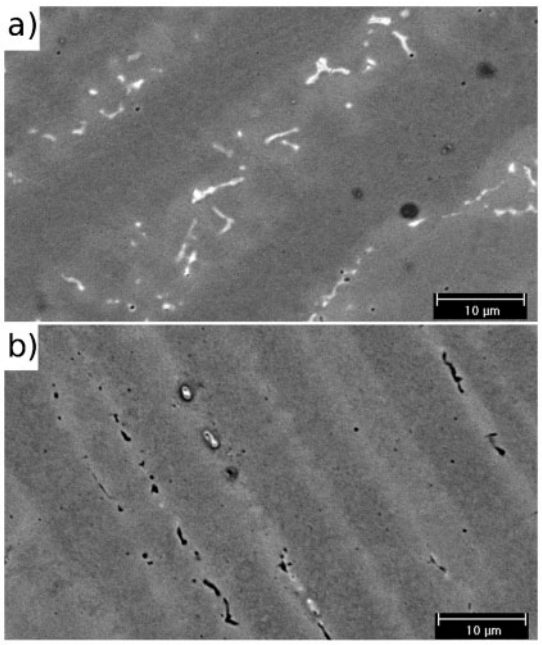

a AWS ER NiCrMo-3 consumable; *b* GSCO 12 consumable

4 Backscaterred electron micrographs of fusion zone

Residual stress distribution and distortion

Figure 5*a* shows the longitudinal and transversal stress distribution measured by X-ray diffraction in sample welded using nickel based alloy. The maximum tensile residual stresses were found in the fusion zone with peak stresses of 300 MPa in longitudinal and 290 MPa in transversal direction, respectively. In the fusion zone, tensile residual stress band (~12 mm in width), was measured in longitudinal and transversal directions. Further away from the welded region, a compressive stress develops in both the heat affected zone (HAZ) and unaffected parent material to balance the tensile stress which fades away to zero towards the edge of the plate.

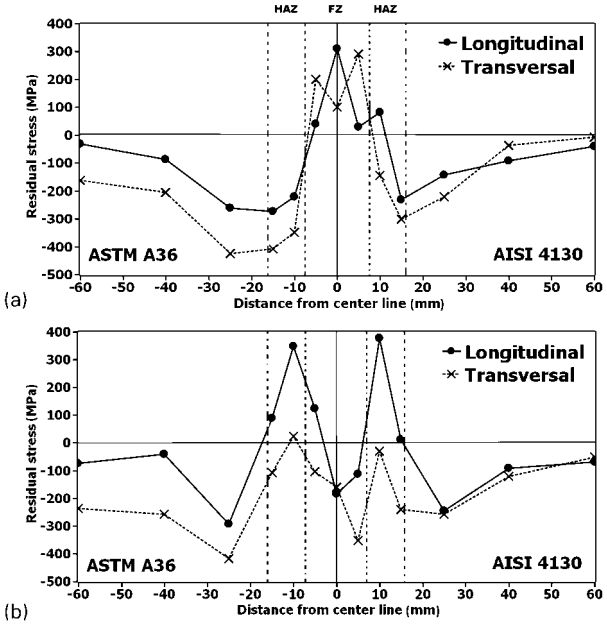

5 Residual stress distribution at top surface in plates welded with *a* AWS ER NiCrMo-3 consumable and *b* GSCO 12 consumable

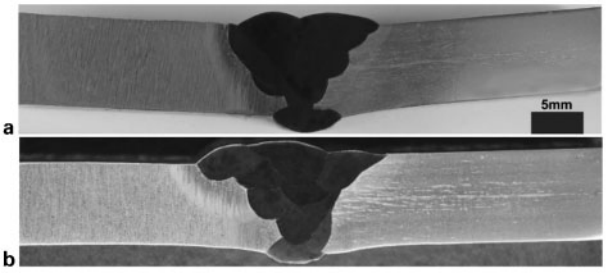

6 Macrograph of specimens welded using *a* AWS ER NiCrMo-3 consumable and *b* GSCO 12 consumable

This is a typically observed residual stresses pattern when a weld consumable with no solid state phase transformation or a high transformation temperature alloy is used.[1] It is to be noted that in order to reduce dilution during welding of dissimilar metals, the AISI 4130 plate was buttered using GSCO12 maraging steel weld consumable prior joining to the ASTM A36 plate with nickel based alloy consumable. No notable effect of buttering on residual stress was observed. This is presumably due to the small thickness of the buttered layer (~2 mm after machining) in addition to a limited number of residual stress measurement points unable to capture residual stress profile in more detail.

Formation of welding residual stresses in two measurement directions for plate welded with GSCO12 maraging 350 steel weld consumable is shown in Fig. 5*b*. In transversal direction, compressive residual stresses were measured with peak value of approximately −400 MPa. In longitudinal direction, a compressive stress band of ~12 mm in width can be observed in the fusion zone with a maximum of around −200 MPa at the weld centreline. At the edge of this band, which corresponds approximately to the fusion zone/HAZ interface, the longitudinal stresses become tensile. The maximum tensile longitudinal stress value, measured in the HAZ at a distance 10 mm from weld centre line, is close to the uniaxial yield strength of the material at the room temperature which is ~400 MPa. At a distance ~15 mm from the weld centreline, compressive longitudinal stresses develop in both the HAZ and unaffected parent material which fades away to zero towards the edge of the plate. In the work performed by Dai *et al.*[26] a similar behaviour was observed. This residual stress pattern can be attributed to a low phase transformation temperature and texture developed during phase transformation and is consistent with references[27–30]. Study of Murakawa *et al.*[27] revealed that the maximum tensile stress at the HAZ/fusion zone interface does not change, whilst the minimum stress in the fusion zone decreases with reduction of transformation start temperature.

Another important observation in the present work was a significantly different magnitude of angular distortion in the two samples Fig. 6. The measured angular distortion in the specimen welded with nickel based alloy consumable was 7° in contrary to 2° in the specimen welded with GSCO12 weld consumable. This kind of distortion is induced by the difference of thermal expansion and shrinkage through the plate thickness. Shrinkage in welded components defines the volume change in the weld region and the heat affected zone as a function of temperature. Since the AWS ER NiCrMo-3

weld consumable does not exhibit any solid state phase transformation the distortion is governed by thermal contraction strains accumulated during cooling of weld metal. In case of GSCO12 maraging 350 steel weld consumable, during cooling of the weld metal, the strain originating from the displacive transformation mechanism compensates for the thermal contraction strains.

Murakawa *et al.*[27] demonstrated that the volume change is larger on cooling when the transformation takes place at lower temperatures. Furthermore, at lower temperatures the accumulated stresses prior to the transformation are likely to be larger, due to the increased yield stress, and this increases the likelihood of transformation plasticity through mechanisms such as variant selection and the Greenwood–Johnson mechanism. A reduction of the magnitude of distortion using a LTT weld consumable is consistent with studies.[30,31]

Conclusions

The following conclusions can be drawn from this work.

1. X-ray diffraction residual stress measurements have shown significant differences between the residual stresses developed in two samples based on use of different weld consumable.

2. A zone of high tensile stresses exists in the fusion zone of the sample A (welded using AWS ER NiCrMo-3 nickel based alloy consumable), whereas most of the fusion zone of the sample B (welded using GSCO12 maraging steel consumable) is in state of compression.

3. A low phase transformation temperature of GSCO12 maraging steel consumable causes compressive stress components to be generated within the fusion zone.

4. Fracture toughness in the fusion zone welded using GSCO12 maraging steel consumable was found to be sufficient.

5. The magnitude of angular distortion in the sample A was higher than in the sample B.

Acknowledgement

The authors are grateful for assistance of Prof. M. P. Cindra Fonseca, A. H. Virgens Neto and D. F. Ribeiro with experiments.

References

1. A. Skouras, A. Paradowska, M. J. Peel, P. E. J. Flewitt and M. J. Pavier: 'Residual stress measurements in a ferritic steel/In625 superalloy dissimilar metal weldment using neutron diffraction and deep-hole drilling', *J. Press. Vessel Technol.*, 2013, **101**, 143–153.
2. V. C. M. Beaugrand, L. S. Smith and M. F. Gittos: 'Subsea dissimilar joints: Failure mechanisms and opportunities for mitigation', Proc. NACE Corrosion, Atlanta, GA, USA, March 2009, TWI, 09305.
3. H. Murakawa, M. Béreš, C. M. Davies, S. Rashed, A. Vega, M. Tsunori, K. M. Nikbin and D. Dye: 'Effect of low transformation temperature weld filler metal on welding residual stress', *Sci. Technol. Weld. Join.*, 2010, **15**, (5), 393–399.
4. W. K. C. Jones and P. J. Alberry: 'A model for stress accumulation in steels during welding', Proc. Conf. on 'Residual stresses in welded construction and their effects', London, UK, November 1977, TWI, Vol. 1, 15–26.
5. P. J. Withers and H. K. D. H. Bhadeshia: 'Residual stress, Part 2: nature and origins', *Mater. Sci. Technol.*, 2001, **17**, 366–375.
6. J. A. Francis, H. J. Stone, S. Kundu, R. B. Rogge, H. K. D. H. Bhadeshia, P. J. Withers and L. Karlsson: 'Transformation temperatures and welding residual stresses in ferritic steels', *Proc. of ASME Press. Vessels Pip. Conf.*, 2008, **6**, 949–956.
7. J. A. Francis, H. J. Stone, S. Kundu, H. K. D. H. Bhadeshia, R. B. Rogge, P. J. Withers and L. Karlsson: 'The effects of filler metal transformation temperature on residual stresses in a high strength steel weld', *J. Press. Vessel Technol.*, 2009, **131**, 041401.1.
8. S. Kundu and H. K. D. H. Bhadeshia: 'Transformation texture in deformed stainless steel', *Scr. Mater.*, 2006, **55**, (9), 779–781.
9. E. J. McDonald, K. R. Hallam, W. Bell and P. E. J. Flewitt: 'Residual stresses in a multi-pass CrMoV low alloy ferritic steel repair weld', *Mater. Sci. Eng. A*, 2002, **A325**, (1–2), 28, 454–464.
10. A. A. Shirzadi, H. K. D. H. Bhadeshia, L. Karlsson and P. J. Withers: 'Stainless steel weld metal designed to mitigate residual stresses', *Sci. Technol. Weld. Join.*, 2009, **14**, 559–565.
11. A. F. Mark, J. A. Francis, H. Dai, M. Turski, P. R. Hurrell, S. K. Bate, J. R. Kornmeier and P. J. Withers: 'Evolution of local material properties and residual stress in a three-pass SA508 steel weld', *Acta Mater.*, 2012, **60**, 3268–3278.
12. J. Altenkirch, J. Gibmeier, A. Kromm, Th. Kannengiesser, Th. Nitschke-Pagel and M. Hofmann: 'In situ study of structural integrity of low transformation temperature (LTT)-welds', *Mater. Sci. Eng.*, 2011, **528**, 5566–5575.
13. A. Ohta, K. Matsuoka, N. T. Nguyen, Y. Maeda and N. Suzuki: 'Fatigue strength improvement of lap joints of thin steel plate using low-transformation-temperature welding wire', *Am. Weld. J.*, 2003, **82**, 78–83.
14. A. Ohta, N. Suzuki, Y. Maeda, K. Hiraoka and T. Nakamura: 'Superior fatigue crack growth properties in newly developed weld metal', *Int. J. Fatigue*, 1999, **21**, 113–118.
15. W. X. Wang, L. X. Huo, Y. F. Zhang, D. P. Wang and H. Y. Jing: 'New developed welding electrode for improving the fatigue strength of welded joints', *J. Mater. Sci. Technol.*, 2002, **18**, (6), 527–531.
16. Ph. P. Darcis, H. Katsumoto, M. C. Payares-Asprino, S. Liu and T. A. Siewert: 'Cruciform fillet welded joint fatigue strength improvements by weld metal phase transformations', *Fatigue Fract. Eng. Mater. Struct.*, 2008, **31**, 125–136.
17. L. Karlsson and L. Mráz: 'Increasing fatigue life with low transformation temperature (LTT) welding consumables', *Zváranie Svarováni*, 2011, **1**–**2**, 8–15.
18. S. Zenitani, N. Hayakawa, J. Yamamoto, K. Hiraoka, Y. Morikage, T. Yauda and K. Amano: 'Development of new low transformation temperature welding consumable to prevent cold cracking in high strength steel welds', *Sci. Technol. Weld. Join.*, 2007, **12**, 516–522.
19. J. Eckerlid, T. Nilsson and L. Karlsson: 'Fatigue properties of longitudinal attachments welded using low transformation temperature filler', *Sci. Technol. Weld. Join.*, 2003, **8**, 353–359.
20. M. Farman, A. ul Haq, Q. R. Ali and A. Q. Khan: 'The origin and influence of residual magnetism on the electron beam welding of 18% Ni-maraging steels', *Mater. Des.*, 1988, **9**, (5), 263–271.
21. ASTM A36 Stell Plate, MatWeb Property Data, http://www.matweb.com/search/DataSheet.aspx?MatGUID=afc003f4fb40465fa3df05129f0e88e6
22. AISI 4130 steel, MatWeb Property Data, http://www.matweb.com/search/datasheet.aspx?MatGUID=ac4f5d552075496692556 3d4437e07a6&ckck=1
23. Maraging 350, Dynamic Metals International, LLC, http://www.dynamicmetals.net/VascoMaxCatalog.pdf
24. Alloy 625, NiWire Industries Co., Ltd., http://www.niwire.com/uploads/documents/ERNiCrMo-3.pdf
25. E. Macherauch and P. Müller: *Z. Angew. Phys.*, 1961, **7**, 305–312.
26. H. Dai, J. A. Francis, H. J. Stone, H. K. D. H. Bhadeshia and P. J. Withers: 'Characterizing phase transformations and their effects on ferritic weld residual stresses with X-rays and neutrons', *Metall. Mater. Trans. A*, 2008, **39A**, 3070–3078.
27. H. Murakawa, M. Béreš, A. Vega, S. Rashed, C. M. Davies, D. Dye and K. M. Nikbin: 'Effect of phase transformation onset temperature on residual stress in welded thin steel plates', *Trans. JWRI*, 2008, **37**, (2), 75–80.
28. J. Yamamoto, Y. Muramatsu, S. Zenitani, N. Hayakawa and K. Hiraoka: 'Control of welding residual stress by low-temperature transformation welding consumables – influence of restraint of joint and transformation temperature on residual stress', Proc. 6th Int. Conf. on 'Trends in welding research', 902–905; 2002, Materials Park, OH, ASM International.
29. M. C. Payares-Asprino, H. Katsumoto and S. Liu: 'Effect of martensite start and finish temperature on residual stress development in structural steel welds', *Weld. J.*, 2008, **87**, 279–289.
30. H. K. D. H. Bhadeshia: 'Possible effects of stress on steel weld microstructures', in 'Mathematical modelling of weld phenomena', (ed. H. Cerjak), Vol. 2, 71–119; 1998, London, Institute of Materials.
31. Y. Mikami, Y. Morikage, M. Mochizuki and M. Toyoda: 'Angular distortion of fillet welded T joint using low transformation temperature welding wire', *Sci. Technol. Weld. Join.*, 2009, **14**, 97–105.